Available online at www.sciencedirect.com
SCIENCE DIRECT®
Precision Engineering 30 (2006) 63–70
PRECISION ENGINEERING
www.elsevier.com/locate/precision

Repeatable and accurate assembly of X-ray foil optics

Craig R. Forest*, Matthew Spenko, Yanxia Sun, Alexander H. Slocum, Ralf K. Heilmann, Mark L. Schattenburg

Massachusetts Inst. of Technology, Center for Space Research, Cambridge, MA 02139, USA

Received 11 October 2004; received in revised form 26 April 2005; accepted 6 May 2005
Available online 18 July 2005

Abstract

Repeatable and accurate assembly of thin, foil optics is crucial to meeting performance goals in optical systems such as grazing-incidence X-ray telescopes and diffractive lithography tools. Our previous work in proving key technologies for assembly has been motivated by the need to meet spectral resolution goals for the NASA *Constellation-X* mission. We report a new generation of technology that makes strides towards simulating actual telescope assembly conditions. Our technology is based on the use of micromachined silicon tooling that we call microcombs. Theoretical error budgeting and analytical models were applied to a mechanical design with an isolated metrology frame and high-resolution actuation with feedback. Experimental testing has yielded assembly results with sub-micron repeatability and accuracy. For complete foil reassembly, placement errors are approximately 0.3 μm over a 140 mm × 100 mm × 0.4 mm foil. Accuracy of assembly in pitch and yaw are 0.34 and 2.01 μm, respectively. This performance meets the 1 μm telescope assembly accuracy goal with the exception of yaw accuracy, which is under continued development.

Keywords: X-ray telescopes; Reflection gratings; Constellation-X; X-ray foil optics; Mirror alignment

1. Introduction

The proposed reflection grating spectrometer (RGS) on the NASA *Constellation-X* mission is designed to provide high-resolution spectroscopy of astrophysical sources in the 0.5–3.5 nm X-ray band. Two types of reflection grating geometries have been proposed for the RGS [2]. In-plane gratings have relatively low-density rulings (∼500 lines/mm) with lines perpendicular to the plane of incidence, thus dispersing X-rays into the plane. Off-plane, or conical, gratings require much higher density rulings (>5000 lines/mm) with lines quasi-parallel to the plane of incidence, thus dispersing X-rays perpendicular to the plane. Both types present unique challenges and advantages and are under intensive development. In both cases, however, grating flatness and assembly tolerances are driven by the mission's high spectral resolution goals and the relatively poor resolution of the Wolter foil optics of the spectroscopy X-ray telescope (SXT) that is used in conjunction with the RGS. In general, to achieve high spectral resolution, both geometries require lightweight grating substrates with arcsecond flatness and assembly tolerances. This implies sub-micron accuracy and precision which go well beyond that achieved with previous foil optic systems. Grating shaping [3] and patterning [4,5] have been previously reported. Here we report on technology development for the assembly of thin, flat grating substrates.

Depending on the particular grating geometry, grating substrates are generally rectangular with dimensions of 100–200 mm and thicknesses from 0.4 to 2 mm. A variety of substrate materials have been proposed including glass, silicon, and silicon carbide. These foil geometric specifications are driven by the telescope weight budget, effective collecting area, and assembly technology. The mission plan includes up to 25 flight "modules," each holding 120 optic foil mirrors or, alternatively, 100 flight "modules" with 20 mirrors each.

As a proof-of-concept, we seek to assemble these optic foils parallel to each other with tolerances that correspond to a 2 arcsec telescope resolution. This implies repeatable and accurate alignment of the front faces of the foils to within 1 μm of their intended positions. This telescope assembly technology, while intended primarily for the assembly of flat

* Corresponding author. Tel.: +1 617 258 0533; fax: +1 617 252 1849.
E-mail address: cforest@mit.edu (C.R. Forest).

0141-6359/$ – see front matter © 2005 Elsevier Inc. All rights reserved.
doi:10.1016/j.precisioneng.2005.05.003

grating substrates, may also find utility in the assembly of Wolter X-ray optics, which utilize parabolic and hyperbolic mirrors with similar geometric specifications and assembly tolerances to the grating substrates.

2. Previous assembly research

2.1. Assembly procedure

The foil alignment tolerances for the NASA *Constellation-X* mission go well beyond those of previous segmented foil optic telescopes. To meet these tolerances, we previously reported a novel assembly scheme [1,6]. In this process, depicted in Fig. 1, a group of optic foils are first loosely held inside a flight module. The flight module is then inserted into precision assembly tooling, where the foils are manipulated into aligned positions and then bonded in place. The flight module is then removed from the assembly tooling. The advantage of this procedure is that the flight module has relaxed tolerance requirements while the precision assembly tooling can be reused. Other telescope assembly work has utilized high accuracy attachment rails for the optics, each being required to maintain sub-micron accuracy [7,8].

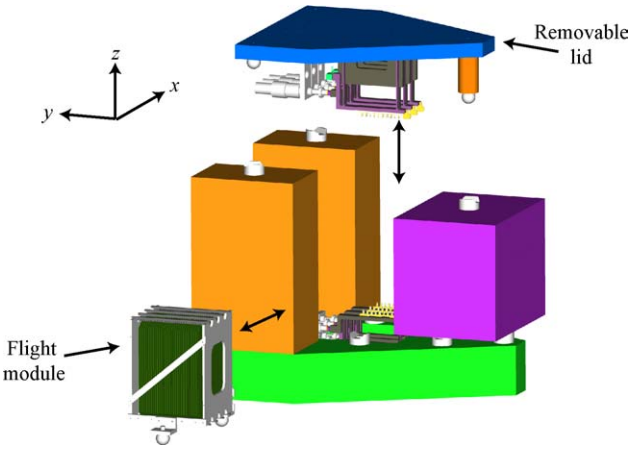

Fig. 1. Depiction of the assembly truss. The lid can be removed to allow insertion of the flight module which loosely holds the foils. Precision tooling then aligns the foils. After bonding, the truss can be reused.

2.2. Microcombs

Within the precision assembly tooling, a set of silicon microstructures, called microcombs, are used to perform the alignment. These high-accuracy silicon microcombs come in two types: reference microcombs and spring microcombs. In the design, the reference microcombs come into contact with a reference flat. The teeth of the reference microcombs then form accurate reference surfaces for the optic foils to register against. This detail is illustrated in Fig. 2. The spring microcombs are then actuated to provide sufficient force to push the foils against the reference microcombs [1,6]. The engineering design of these microcombs has been studied by Mongrard [1] and the complexities of their manufacture have been pioneered by Chen et al. [9,10] and later improved by Sun et al. [11].

In the current work, we have improved the microcombs' design to reduce assembly accuracy degradation due to microcomb rotational errors. If the microcombs are installed in the assembly truss with an unintentional pitch error, the vertical distance from contact point between the comb and flat

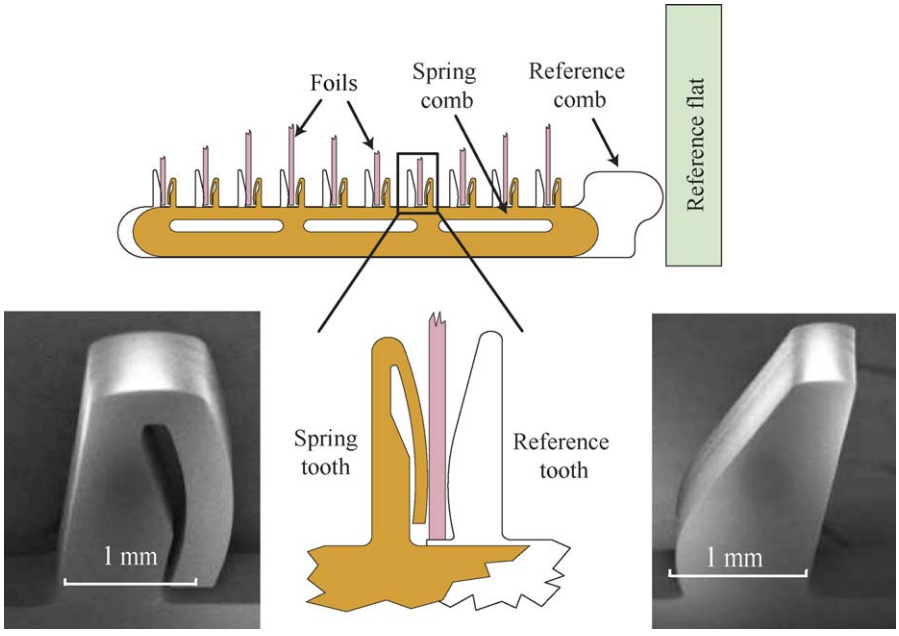

Fig. 2. Foils are forced into alignment by the spring microcombs against the reference microcombs. The reference microcombs are registered against the reference flat surface.

to the contact point between the comb and foil will act as a lever arm for amplifying the comb-to-flat perpendicularity error. This Abbé error can be eliminated if the combs are designed to make the comb-to-flat contact point collinear with the comb-to-foil contact point in the direction of the comb's axis, as shown in Fig. 2.

2.3. Evaluation of previous work

Previous work demonstrated proof-of-concept for the assembly scheme [1,6]. Optic foils were placed repeatedly in slots against various reference teeth in a rigid assembly truss to compare the repeatability for the same slot and the accuracy between different slots and the reference flat. This research proved that the microcombs have the potential to provide accurate and repeatable reference surfaces for segmented foil optics. The current work more closely simulates actual telescope assembly conditions.

3. Assembly truss design

The redesigned assembly truss is shown in Fig. 3. Four key features shall be discussed in more detail: the reference flat, kinematic couplings, flight module, and flexure bearing assemblies. In addition, the flexure bearing assembly was modeled to predict the dynamic performance of the system.

3.1. Reference flat

The reference flat is shown in relation to the assembly truss in Fig. 4. This part is a solid block of 6061-T6 aluminum plated with 125 μm of electroless nickel to resist scratching during use. One face of the block is lapped and optically polished to 1.5 μm peak-to-valley (P–V) flatness as measured with a Shack-Hartmann metrology system [12].

3.2. Kinematic couplings

Ball and vee-block kinematic couplings were selected to allow repeatable placement of the flight module onto the base, the reference flat onto the base, and the cover onto the reference flat and base. One of these couplings is shown enlarged in Fig. 4. Kinematic couplings of this design and application have sub-micron repeatability [13]. The vee-blocks are oriented to ensure uniform load distribution and prevent the vee-block faces from over-constraining the parts.

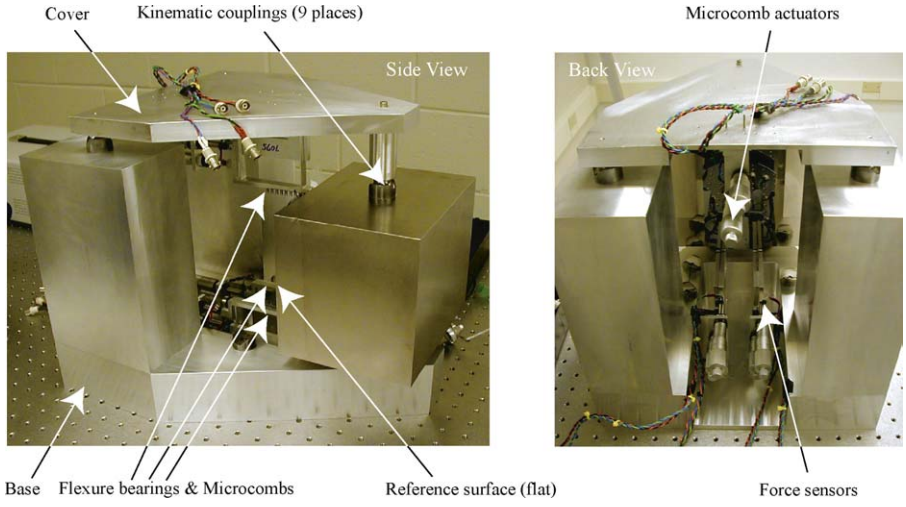

Fig. 3. Photographs of foil optic assembly truss. The flight module is not inside of the assembly truss for this figure.

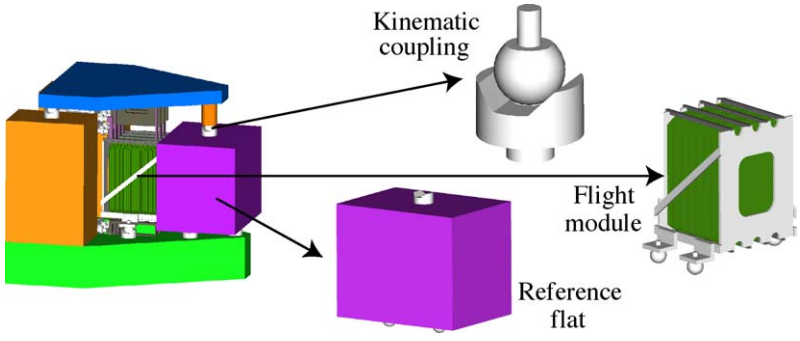

Fig. 4. Depiction of assembly truss reference flat, kinematic couplings, and flight module. The kinematic couplings are located at nine distinct positions on the truss to repeatably orient the reference flat, cover, and flight module.

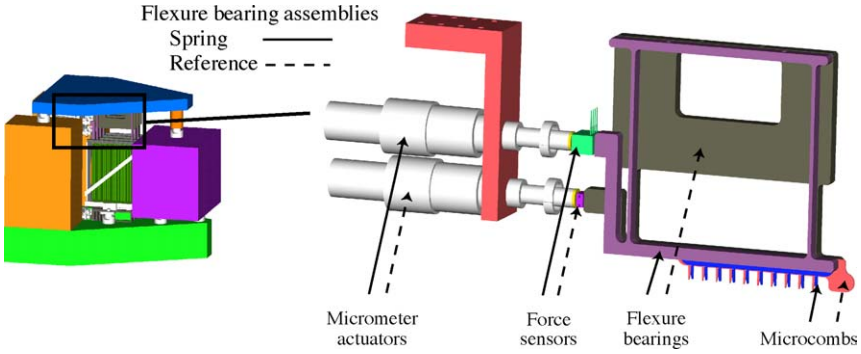

Fig. 5. Depiction of the flexure bearing assembly containing microcombs, flexure bearings, force sensors, and micrometers.

3.3. Flight module

The flight module, shown in Fig. 4, is designed to hold 30 foils loosely in a set of "coarse combs" before assembly. The microcombs manipulate the foils into their aligned locations within the oversized slots of these coarse combs. After the foils are aligned, glue is injected into the coarse comb slots to secure the foils in place.

3.4. Flexure bearing assemblies

The heart of the assembly truss is the flexure bearing assembly, shown in Fig. 5. The flexure bearings provide independent, hysteresis-free, friction-free support for the reference combs to make contact with the reference flat and for the spring combs to impart forces to the foils. The four-bar linkage design of the flexure bearings allows parallel motion between the top and bottom members. The parasitic pitch error in this motion is virtually eliminated with proper selection of the position of the driving point [14]. The flexures are actuated at half of their height by differential screw micrometers (Mitutoyo model 110–102) which have a resolution of 0.1 μm. This resolution is necessary to achieve the microcomb placement accuracy of 1 μm. Force sensors (Honeywell models LPM 560, LPM 562 sold by Cooper Instruments) are placed between the micrometers and the flexure bearings. These sensors allow detection of contact with the reference flat, since upon contact the stiffness of the system changes. Before contact, the force per unit displacement is a function of the stiffness of the flexure bearings, force sensors, micrometers, and micrometer holders. After contact, there is an additional stiffness component due to Hertzian deformation at the microcomb/reference-flat interface.

Mathematical modeling was performed [15] to aid in the design of the flexure bearing assembly. The details are omitted, except to briefly discuss the design objectives. This modeling was undertaken for two purposes: (1) The system stiffness will change after contact with the reference flat. We designed the flexure bearing assembly so that this change in stiffness is well defined and can be easily measured. (2) We desired that the micrometer bracket flex backwards after contact, thus acting as a relief, preventing microcomb nose fracture.

4. Microcomb contact with reference flat, experimental

The flexure bearing assembly is actuated until the microcomb makes contact with the reference flat, as shown in Fig. 6. The stiffness plot in Fig. 7 reveals when contact with the reference flat has occurred. The contact location can easily and repeatably be resolved to <1 μm of actuator displacement. To compare with the mathematical modeling of the stiffness, the force per displacement slopes from several flexure bearing assemblies were measured, as shown in Table 1.

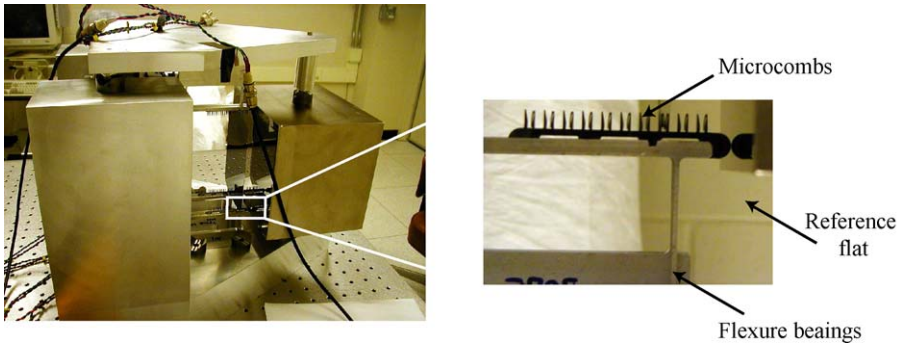

Fig. 6. Assembly truss during testing with reflective optic foil inserted. The microcomb is in contact with the reference flat (inset).

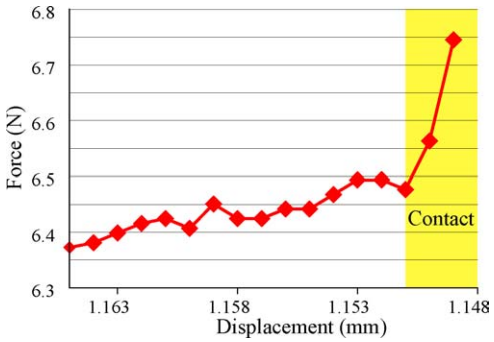

Fig. 7. Experimental data from the flexure bearing assembly. Contact with the reference flat is observable from the dramatic change in slope.

Table 1
Stiffness measurements from flexure bearing assembly compared with theory

	Before contact stiffness, $k_{<c}$ (10^3 N/m)	After contact stiffness, $k_{>c}$ (10^3 N/m)
Theory	8.2	116.0
Experimental	10.5±2.1	109.8±32.8
% Difference	29%	5%

The theoretical and experimental values compare reasonably well.

5. Repeatability testing

Numerous tests have been performed on the assembly truss to determine its ability to meet precision foil alignment goals of 1 μm. An autocollimator (Newport, model LAE500H) was used to measure the angular errors of a foil located in a "slot," which were then converted to displacements. Previous experiments performed on a static breadboard test assembly system have demonstrated a 1 σ mounting slot repeatability error of about 0.11 μm in both axes [16]. This previous research defined repeatability as the standard deviation of a set of measurements collected by successively measuring, lifting, and replacing a fused-silica plate against fixed reference microcomb teeth. This test was repeated with the new design and the data shows less than 0.05 μm for both pitch and yaw.

The current research involves a dynamic assembly truss, which strives to mimic the actual telescope foil alignment procedures. The procedure for the repeatability test is as follows: a single foil was slid from the side of the assembly truss into a microcomb slot and preloaded by gravity against the microcombs. Reference microcombs were then driven into contact with the reference flat. Pitch and yaw of the foil were recorded with an autocollimator zeroed to the reference flat. The combs were then retracted, and the assembly truss lid was raised and replaced. The reference combs were then driven back into contact with the flat, and the foil angle was recorded. This procedure was repeated three times for both a 3 mm-thick quartz plate coated with 100 nm of aluminum and a 0.4 mm-thick silicon wafer, both of size 140 mm × 100 mm. Results from these tests are summarized in Table 2.

Table 2
Assembly truss single slot repeatability results

Displacement error, one σ (μm)			
0.4 mm-thick silicon wafer		3 mm-thick fused-silica plate	
pitch	yaw	pitch	yaw
0.34	0.36	0.33	0.30

Displacement error is the displacement of the edge of the foil extracted from its angular error and dimensions.

6. Accuracy testing

The accuracy of foil placement in the assembly truss has also been measured. In these tests, we compared the angular error of the foil with respect to the reference flat after the microcomb length errors have been subtracted. This compensation was necessary due to fabrication errors in the microcombs. For these experiments, the 3 mm-thick quartz plate was used to measure system accuracy.

The accuracy terms we will use are conveyed in Fig. 8. The terms θ_{mi} and ϕ_{mi} refer to measured yaw (θ) and pitch (ϕ) of the foil for measurement number i. We seek the average systematic error in the device, θ_s and ϕ_s with respect to the reference the reference flat, converted to linear dimensions, as a measurement of the accuracy.

There are three microcombs and three possible microcomb positions, so six permutations of the combs are possible. In the accuracy testing procedure, the lid was placed on the assembly truss, the foil was inserted, the combs were driven into contact with the flat, and the foil's angular orientation was measured with the autocollimator. The truss was then disassembled, the flexure bearing assemblies were permuted, and the assembly procedure was repeated. Six comb permutations resulted in six foil angular pitch and yaw measurements. This entire process was repeated for three different slots in the microcombs.

The systematic yaw error, θ_s, can be defined, according to Fig. 8, as

$$\theta_s = \theta_{m1} - \frac{L_1 - L_2}{d}. \tag{1}$$

For the systematic pitch error, ϕ_s, we derive a similar expression

$$\phi_s = \frac{\phi_{m1} + \phi_{m2}}{2} + \frac{1}{H}\left(L_3 - \frac{L_1 + L_2}{2}\right), \tag{2}$$

where the measurements ϕ_{mi} are averaged in Eq. (2) since there is no new information gained by the permutations of comb L_1 and L_2. Thus, there are only three unique equations for ϕ_s.

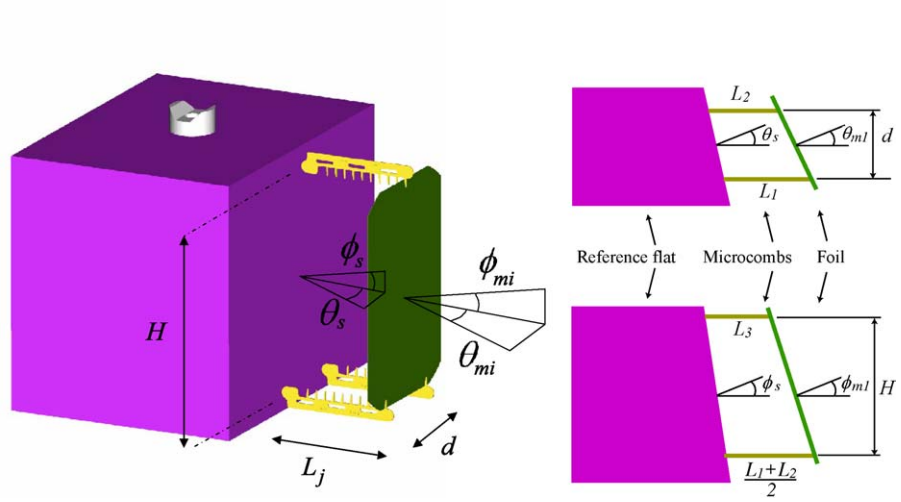

Fig. 8. Accuracy testing coordinate systems. $d = 55$ mm, $H = 140$ mm. Cross sections illustrate the relationship between comb lengths and angular quantities.

Combining Eqs. (1) and (2) into the form $Ax = b$ yields

$$\begin{bmatrix} 1 & -1 & 0 & 1 & 0 \\ -1 & 1 & 0 & 1 & 0 \\ -1 & 0 & 1 & 1 & 0 \\ 1 & 0 & -1 & 1 & 0 \\ 0 & 1 & -1 & 1 & 0 \\ 0 & -1 & 1 & 1 & 0 \\ 1 & 1 & -2 & 0 & 2 \\ 1 & -2 & 1 & 0 & 2 \\ -2 & 1 & 1 & 0 & 2 \end{bmatrix} \begin{bmatrix} L_1 \\ L_1 + L_2 \\ L_1 + L_3 \\ d \cdot \theta_s \\ H \cdot \phi_s \end{bmatrix} = \begin{bmatrix} d \cdot \theta_{m1} \\ d \cdot \theta_{m2} \\ d \cdot \theta_{m3} \\ d \cdot \theta_{m4} \\ d \cdot \theta_{m5} \\ d \cdot \theta_{m6} \\ H \cdot (\phi_{m1} + \phi_{m2}) \\ H \cdot (\phi_{m3} + \phi_{m4}) \\ H \cdot (\phi_{m5} + \phi_{m6}) \end{bmatrix}. \quad (3)$$

The linear system of equations is overconstrained, so we perform a least squares fit [17]. Solving this least squares equation results in

$$x = (A^{\mathrm{T}}A)^{-1}A^{\mathrm{T}}b. \quad (4)$$

Only the relative comb lengths can be found using an autocollimator, as indicated by the equations. This procedure was repeated for three different slots.

The resulting systematic errors for these three slots is shown along with average values in Table 3. Discussion of these results follows in Section 8.

Table 3
Assembly truss slot accuracy results

	Yaw $d \cdot \theta_s$ (μm)	Pitch $H \cdot \phi_s$ (μm)
Slot 1	0.56	−1.84
Slot 2	0.25	−1.84
Slot 3	0.21	−2.34
Avg	0.34	−2.01

Displacement error is the displacement of the edge of the foil extracted from its angular error and dimensions. The errors for three successive slots are shown along with the average systematic angular errors.

7. Error budget

An error budget was performed for the assembly truss design. This theoretical error budget carefully tracked the errors in every part leading from a reference frame located at the center of the reference flat face to the point-of-action, the contact interface between the microcomb and foil [15]. The error budget table and the summarized results are presented in Table 4. Coordinate system orientation is indicated in Fig. 1.

8. Discussion

The repeatability results meet the functional requirements for the assembly of foil optics. These ∼0.3 μm repeatability errors could be further reduced by improving autocollimator measurement repeatability and eliminating Hertzian deformations at the comb/reference flat interface and comb/foil interface. Comparing the difference in the final test results for the different foil thicknesses, thin foil deformation does not appear to be a significant contributor to the overall error.

The error budget predicts that the expected accuracy of the assembly truss alignment is 0.5 μm in pitch and yaw, assuming that systematic error can be recorded and compensated. The errors are nearly identical in the three microcombs due to the symmetric structure of the assembly truss. These results

Table 4
(*Top*) Error budget table and (*bottom*) results in the sensitive direction, *Y*, for the assembly truss design

Axes	Actual Dim.	Rand. errors	Sys. errors	Error description
Errors for CS located at contact point between comb and ref. flat (CS_2) to ref. CS.				
X (mm)	28	0.0381	0	Root-sum-squared (RSS) contributions: 0.0127 mm error of kinematic coupling hole placement, 0.0254 mm flexure bearing hole placement, 0.0254 mm variation in flexure bearing thickness.
Y (mm)	0	0.0001	0.0003	Rand: RSS contributions: 0.0001 mm flatness of reference flat, 35 μm deformation of reference flat due to Hertzian compression. Sys: thickness variation of the foils induces Hertzian deformation on the comb teeth.
Z (mm)	−74	0.0508	0	RSS contributions: tolerance in height of kinematic couplings, machining tolerances on lid, flexure bearings, alignment of combs to flexure bearings, sag in lid due to gravity.
θ_X (rad)	0	0.0004	0	RSS contributions: reference flat perpendicularity; flatness and parallelism for flexure bearings, base, lid; pitch error of the flexure bearings upon actuation.
θ_Y (rad)	0	0.0040	0	RSS contributions: flatness and parallelism of lid and flexure bearings.
θ_Z (rad)	0	0.001	0	Angular errors due to hole placement in base and flexure bearings.
Errors for CS located at contact point between comb and foil (CS_1) to CS_2.				
X (mm)	0	0.0005	0	Variation in comb thickness. Manufacturer specification for wafer thickness is 475±0.25 μm
Y (mm)	70	0.0004	0	Tolerances on comb manufacturing estimated as 0.5 μm per 100 mm of length.
Z (mm)	0	0	0	Distance from the centerline CS_1 to CS_2 = 0 mm.
θ_X (rad)	0	0	0	Angular errors accounted for in the Z direction.
θ_Y (rad)	0	0.0005	0	Silicon wafer bow results in curling of the combs. Worst wafer flatness measured using Hartmann metrology tool was 5 μm over a 10 mm half period.
θ_Z (rad)	0	0.0005	0	Same description as $\theta_{Y\text{random}}$
			Average sum and Root-sum-squared (RSS) random errors (μm)	Net total systematic errors (μm)
			0.5	0.3

The reference coordinate system (CS) is located at the center of the reference flat face.

predict that the foil should be aligned in pitch and yaw to within 0.5 μm in the as-built machine. This is a purely theoretical estimation, and the errors could be better or worse depending on the particular milling machine used to make the parts, wafer warp, etc. Comparing them to the accuracy testing results in Table 3, we see that the prediction is close. In yaw, the difference is less than 0.2 μm. This indicates that with better manufacturing tolerances and a revised error budget, accuracy should further improve.

In pitch, the experimental errors are greater than the prediction by approximately 1.5 μm. Some sources of error in the accuracy measurements are that the reference flat was only polished to 1.5 μm P–V and that the quartz "optic" was only flat to 2 μm P–V. The linear systematic errors in Table 3 correspond to an angular systematic error of 2.95 arcsec in pitch and 1.13 arcsec in yaw. Therefore, this device meets the 2 arcsec assembly functional requirement for accuracy in yaw. The pitch error is beyond the functional requirement. However, with better polishing of the reference flat and optics with less warp, this error may be within the specification. We also expect systematic errors in the microcombs to be reduced with a revised manufacturing process [18]. The design and performance of the assembly truss meets the requirements from Sec. 1, with the notable exception of the systematic pitch error previously described.

9. Conclusions

Major advances over previous optical assembly research have been achieved. The assembly tool design enables microcomb actuation to repeatably and accurately position the optic foils. Realistic optic foil sizes and materials have been assembled. The design integrates an independent flight module, which holds the foils loosely before alignment, and will permit an adhesive to secure the aligned foils for future work. The design permits the flight module to be repeatably constrained within the assembly truss. Errors in the assembly tooling have been quantified theoretically and compared to experimental results. The closed structural loop is stiff and the metrology frame is effectively decoupled from it. Active feedback in the form of force sensing enables continuous monitoring of the state of the foil boundaries. Thus, this assembly tool development has enabled substantial progress toward successful assembly of foil optics for NASA's X-ray telescope mission.

Acknowledgments

The support of the students, staff, and facilities from the Space Nanotechnology Laboratory are much appreciated.

This work is supported by NASA Grants NAG5-12583 and NAG5-5404 and the National Science Foundation.

References

[1] Mongrard O. High accuracy foil optics for X-ray astronomy. Master's thesis. Massachusetts Institute of Technology. Dept of Aeronautics and Astronautics; 2001.
[2] Rasmussen A, Aquila A, Bookbinder J, Chang C, Gullikson E, Heilimann RK, et al. Grating arrays for high-throughput soft X-ray spectrometers. Proc SPIE 2004;5168:248–259.
[3] Heilmann RK, Monnelly GP, Mongrard O, Butler N, Chen CG, Cohen LM, et al. Novel methods for shaping thin-foil optics for X-ray astronomy. Proc SPIE 2002;4496:62–72.
[4] Franke AE, Schattenburg ML, Gullikson EM, Cottam J, Kahn SM, Rasmussen A. Super-smooth X-ray reflection grating fabrication. J Vac Sci Technol B 1997;15(6):2940–5.
[5] Chang C-H, Heilmann RK, Fleming RC, Carter J, Murphy E, Schattenburg ML, et al. Fabrication of saw-tooth diffraction gratings using nanoimprint lithography. J Vac Sci Technol B 2003;21(6):2755–59.
[6] Monnelly GP, Mongrard O, Breslau D, Butler N, Chen CG, Cohen LM, et al. High-accuracy X-ray foil optic assembly. Proc SPIE 2000;4138:164–73.
[7] Montesanti RC, Davis PJ. Fabrication of the attachment rails used for mounting an array of eight X-ray reflection gratings. Proc ASPE 1993;8:158–61.
[8] Montesanti RC. Inspection of the diamond-turned surfaces used for mounting an array of eight X-ray reflection gratings. Proc ASPE 1993;8:374–7.
[9] Chen CG, Heilmann RK, Konkola PT, Mongrard O, Monnelly GP, Schattenburg ML. Microcomb design and fabrication for high accuracy optical assembly. J Vac Sci Technol B 2000;18(6):3272–6.
[10] Chen CG. Microcomb fabrication for high accuracy foil X-ray telescope assembly and vector Gaussian beam modeling. Master's thesis. Massachusetts Institute of Technology. Dept of Electrical Engineering and Computer Science; 2000.
[11] Sun Y, Chen CG, Heilmann RK, Forest C, Spenko M, Konkola PT, et al. Precision microcomb design and fabrication for Constellation-X soft X-ray telescope segmented optic assembly. Proc ASPE 2002;27:261–6.
[12] Forest CR, Canizares CR, Neal DR, McGuirk M, Schattenburg ML. Metrology of thin transparent optics using Shack-Hartmann wavefront sensing. Optical Eng 2004;43(3):742–53.
[13] Culpepper ML, Slocum AH, Shaikh FZ. Compliant kinematic couplings for use in manufacturing and assembly. Proc ASME IMECE 1998;8:611–8.
[14] Muranaka Y, Inaba M, Asano T, Furukawa E. Parasitic rotations in parallel spring movements. J Jpn Soc Prec Eng 1991;25:208–13.
[15] Forest CR. X-ray telescope foil optics: assembly, metrology, and constraint. Master's thesis. Massachusetts Institute of Technology. Dept of Mechanical Engineering; 2003.
[16] Mongrard O, Butler N, Chen CG, Heilmann RK, Konkola PT, McGuirk M, et al. Proc ASPE 2001;25:40–3.
[17] Strang G. Introduction to applied mathematics. Cambridge: Wellesley; 1986.
[18] Sun Y, Heilmann RK, Chen CG, Forest CR, Schattenburg ML. Precision microcomb design and fabrication for X-ray optics assembly. J Vac Sci Technol B 2003;21(6):2970–2974.